공학석사학위논문

Tetraphenylsilane Containing Solution-Processable Small-Molecular Hosts for Highly Efficient Phosphorescent Organic Light-Emitting Diodes

Tetraphenylsilane 기를 포함하여 용액 공정이 가능한 고효율 인광 유기전계발광소자 단분자 호스트 물질에 관한 연구

2012 년 8 월

서울대학교 대학원

재료공학부

조 명 현

Tetraphenylsilane Containing Solution-Processable Small-Molecular Hosts for Highly Efficient Phosphorescent Organic Light-Emitting Diodes

A THESIS SUBMITTED IN PARTIAL FULFILLMENT OF
THE REQUESTMENTS FOR THE DEGREE OF MASTER
IN ENGINEERING AT THE GRADUATE SCHOOL OF
SEOUL NATIONAL UNIVERSITY

August 2012

BY

Myung-Hyun Jo

Supervisor

Soo Young Park

ABSTRACT

Tetraphenylsilane Containing Solution-Processable Small-Molecular Hosts for Highly Efficient Phosphorescent Organic Light-Emitting Diodes

Myung-Hyun Jo

Department of Materials Science and Engineering

The Graduate School

Seoul National University

In this report, a new series of tetraphenylsilane-functionalized solution-processable, and small-molecular host materials for phosphorescent organic light-

emitting diodes (PhOLEDs) was reported, namely, 9-phenyl-3-(4-(triphenylsilyl)phenyl)-carbazole (TPSPCz), 9-phenyl-3,6-bis(4-(triphenylsilyl)phenyl)-carbazole (TPS_2PCz), 1,2-*trans*-bis(3,6-bis(4-(triphenylsilyl)phenyl)-carbazol-9-yl)cyclobutane (TPS_4DCz). Functionalization of carbazole with tetraphenylsilane (TPS) group leads to significantly enhanced solution-processed thin film formability. From photophysical and morphological study, excimer formation of co-planar carbazole units was successfully suppressed through site-isolation effect of bulky TPS group. As increasing number of TPS group, these hosts exhibit more and more higher thermal decomposition temperatures (TPSPCz : 363 ℃, TPS_2PCz : 424 ℃, TPS_4DCz : 472 ℃), which corresponding to 5% weight loss. Especially, PhOLED comprising green emitting *fac*-tris(2-phenylpyridine) iridium (III) ($Ir(PPy)_3$):TPS_4DCz as a emitting layer, showed superior device performance ($\eta_{c,\,max}$ = 25.10 cd A^{-1}, $\eta_{ext,\,max}$ = 8.95 %) to ($Ir(PPy)_3$):PVK device ($\eta_{c,\,max}$ = 16.51 cd A^{-1}, $\eta_{ext,\,max}$ = 3.52 %).

Keywords : *tetraphenylsilane, solution-process, small-molecule, host materials, phosphorescence, electrophosphorescence, OLED.*

Student number : 2010-20632

TABLE OF CONTENTS

LIST OF FIGURES

CHAPTER I. Introduction

CHAPTER II. Tetraphenylsilane Containing Solution-Processable Small-Molecular Hosts for Highly Efficient Phosphorescent Organic Light-Emitting Diodes

Figure 7 *J-V-L* characteristics of (a) TPS_4DCz:FIrpic device, (c) TPS_4DCz:$Ir(Piq)_2acac$ device and external quantum efficiency and power efficiency versus current density curves for (b) TPS_4DCz:FIrpic device, (d) TPS_4DCz:$Ir(Piq)_2acac$ device.

LIST OF SCHEMES

CHAPTER II. Tetraphenylsilane Containing Solution-Processable Small-Molecular Hosts for Highly Efficient Phosphorescent Organic Light-Emitting Diodes

LIST OF TABLES

CHAPTER II. Tetraphenylsilane Containing Solution-Processable Small-Molecular Hosts for Highly Efficient Phosphorescent Organic Light-Emitting Diodes

Chapter I. Introduction

I-1. Physics of Electrophosphorescence

Photo-excitation molecular emission in visible region is very interesting theme for both their photophysical properties and applications. Light-emissions are divided into two types according to their transition characteristics, namely, fluorescence and phosphorescence. Ground state is excited by photon, electrons at the excited state go down to lowest excited state. Herein, four states are available to be occupied, one singlet state and three triplet states. Fluorescence is the emission that excited electron at the singlet state goes down to the ground state, and phosphorescence is the emission which caused by excited electron at the triplet states.

When an electron and a hole recombine through Coulomb interaction in an organic solid, an excited state of either singlet or triplet is formed. It is generally accepted that simple statistics gives 25% for singlet and 75% for triplet excitons are generated (Figure 1). As previously stated, Electrofluorescence is defined as the radiative recombination of the singlet exciton, while electrophosphorescence is that of triplet exciton.

However, there is a serious limitation in electroluminescent efficiency with using of fluorescent emitters. By the spin-conservation rule, only the singlet excitons can radiative decay to the singlet ground state and the triplet excitons

undergo non-radiative decay. Therefore, the limit of the electrofluorescence efficiency is obviously 25%, provided all excited singlets decay radiatively.

On the other hand, phosphorescent emitters can utilize both singlet and triplet excitons to undergo radiative decay. Thus, we can get 100% internal quantum efficiency by using electrophosphorescence. This means that we can get four times higher electroluminescent efficiency from phosphorescent emitters compared to fluorescent emitters.

By spin-conservation rule, singlet to triplet conversion is forbidden transition. However, using triplet excitons to the radiative decay can be explained by flipping of an electron's spin by spin-orbit coupling mechanism. When we consider quantum mechanical expression of spin-orbit coupling, the spin-orbit coupling energy is given by $E_{SO} = \frac{Z^4}{2(137)^2 n^3}\left(\frac{j(j+1) - l(l+1) - s(s+1)}{2l(l+0.5)(l+1)} \right)$. It is noticeable thing that the spin-orbit coupling increases as the fourth power of the effective nuclear charge Z, but decreases only as the third power of the principal quantum number n. Therefore disadvantage of fluorescent emitters can be overcome by spin-orbit coupling interactions. The spin-orbit coupling is significantly larger for some organic materials, such as transition metal complexes comprising heavy metals.

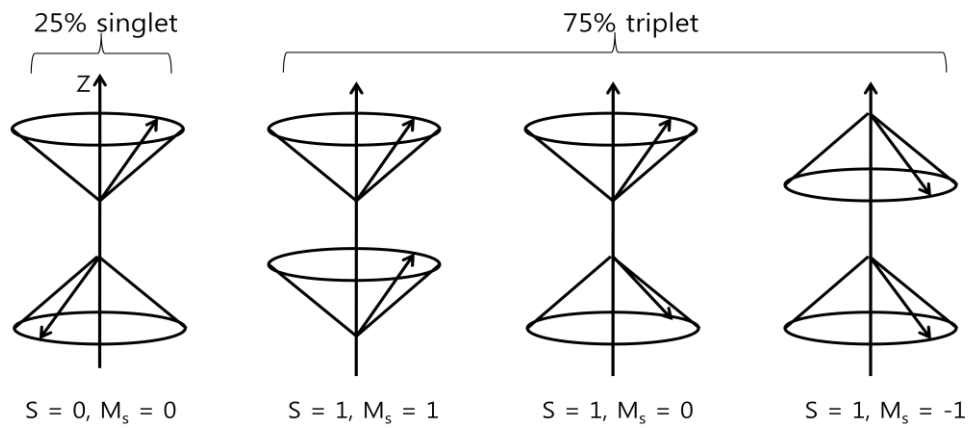

Figure 1. Vector representation of the singlet and triplet states. (taken from reference 1)

I-2. Physics of Electrophosphorescent Light-Emitting Devices

In general, organic layers of organic light-emitting devices are placed between a transparent anode (such as indium tin oxide, ITO) and metallic cathode which has low work function. Electrons and holes are injected from the corresponding electrodes to the organic layers. The charge injection mechanism in electrode/organic material contact can be explained by that in metal/semiconductor contact.

When a metal with work function $q\Phi_m$ is brought in contact with a semiconductor which have a work function $q\Phi_s$, charge transfer occurs until the Fermi levels align at equilibrium (Figure 2 and Figure 3). When a Schottky barrier is formed between the metal and semiconductor (Figure 2), injection of charge carriers from the electrode requires that charges should overcome or tunnel through the barrier. Otherwise, when an Ohmic contact is formed between the metal and semiconductor contact (Figure 3), no contact resistance to overcome the barrier exists.

When there is the Schottky barrier, two possible ways to overcome the barrier are, tunneling and thermionic emission. If the depletion region at the metal-semiconductor interface is thin, carriers can readily tunnel through such barrier. The thermionic emission theory assumes that electrons, which have efficient high thermal energy compared to the barrier, will cross the barrier provided they move towards the barrier.

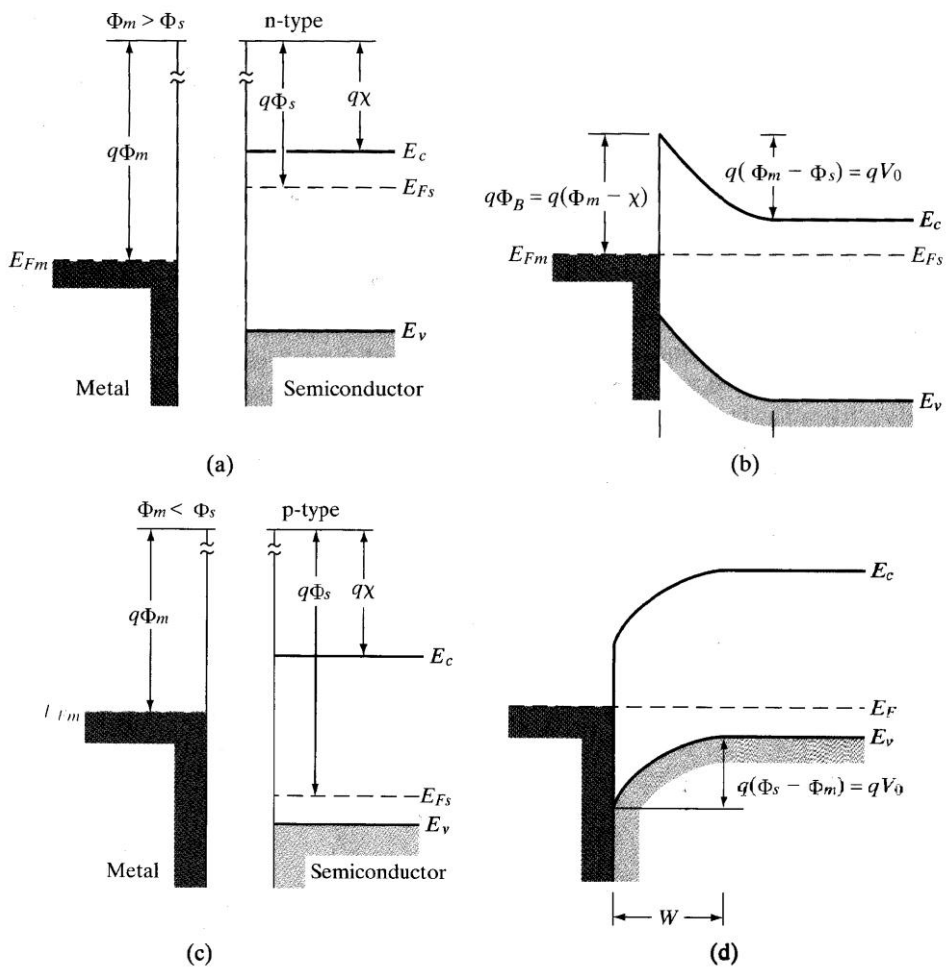

Figure 2 Schottky barrier formed by metal-semiconductor contacts: (a) $\Phi_m > \Phi_s$ for an n-type semiconductor, and (b) the equilibrium band diagram for the junction; (c) $\Phi_m < \Phi_s$ for a p-type semiconductor, and (d) the junction at equilibrium. (taken from reference 2)

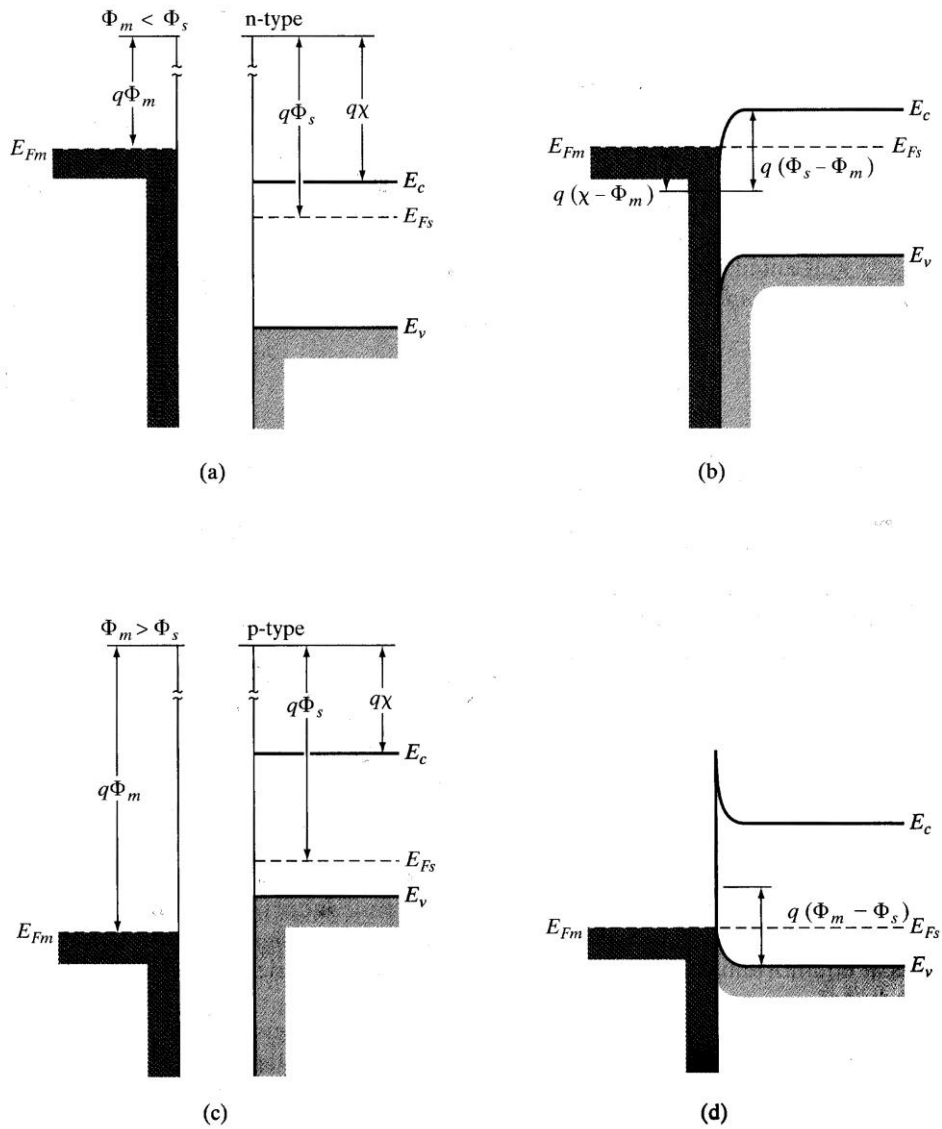

Figure 3 Ohmic metal-semiconductor contacts: (a) $\Phi_m < \Phi_s$ for an n-type semiconductor, and (b) the equilibrium band diagram for the junction; (c) $\Phi_m > \Phi_s$ for a p-type semiconductor, and (d) the junction at equilibrium. (taken from reference 2)

Phosphorescent materials, having relatively longer luminescent lifetime (> ~ms), are prone to be affected by excited-state intermolecular interactions, such as triplet-triplet annihilation,[3] excimer formation.[4] In this regards, phosphorescent organic light-emitting diodes (PhOLEDs) are typically fabricated in a configuration in which the emissive layer is comprised of the phosphors doped in host materials. In other words, choosing appropriate host materials plays an important role to reduce possibility of triplet-triplet annihilation and excimer formation of phosphors.

The charge carriers (holes and electrons) injected and transported from electrodes, form exciton in the host material. Then, excited state energy of host material is transferred to the phosphor by several mechanisms.[5]

A donor in its excited state can transfer energy by a long-range resonant dipole-dipole coupling mechanism to an acceptor. The theory is based on the concept of treating the donor and acceptor as oscillating dipoles that can undergo an energy exchange with dipoles having similar resonance frequency. In this regard, resonance energy transfer is analogues to the behavior of coupled oscillators. Dexter energy transfer is an electron exchange mechanism. Triplet-triplet energy transfer is forbidden by the dipole-dipole mechanism. However, triplet-triplet energy transfer is spin-allowed by the exchange mechanism. Therefore, we expect that triplet-triplet energy transfer will generally occur only through the exchange mechanism. Once the donor molecule is excited, the electrons in the triplet state can be jumped into the triplet state of the acceptor molecule with extinction energy. Simultaneously, electrons in the ground state of the acceptor are transferred to the ground state of the donor material. Only singlet-singlet or triplet-triplet energy

transfer is possible, for the electron-spin must be conserved through electron exchange in Dexter energy transfer process.

I-3. Recent Progress on Solution-Processable Host Materials for Electrophosphorescent Light-Emitting Devices

I-3-1. Solution-Processable Host Materials for Polymer-based PhOLEDs

In this part, the recent progress on phosphorescent dye-dispersed polymer OLEDs will be described. Advances for polymer-based PhOLEDs are currently in progress. One of the main drivers for that is the ultimate realization of high efficiency solution-processed OLEDs based on phosphorescent materials. Effort in this direction can be traced to initial approaches based on fluorescent materials using poly-(methyl methacrylate) (PMMA) matrix.[6] The resulting single organic layer device can substantially reduce the complexity used in multilayer heterostructure OLEDs. This work was extended to the use of poly-(*N*-vinylcarbazole) (PVK) as a host matrix polymer dispersed with different emitters.[7]

The use of phosphorescent dyes dispersed in conjugated polymer systems is realized.[8] However, it was reported that conjugated polymer systems has low triplet energies. One way to overcome this problem of low triplet energy is to alter the linking of monomer units in conjugated polymers. This approach has been attempted to prevent extended conjugation to raise the triplet energies of the polymers. Carbazole-based conjugated polymers with triplet energies as high as 2.6 eV have been realized by this method.[9]

Additionaly, considerable effort has been directed toward the use of small

molecules dispersed in nonconjugated matrix polymer systems.[10]

I-3-2. Solution-Processable Host Materials for Small-Molecule-based PhOLEDs

To simplify the fabrication techniques process, much research effort has been devoted to develop PhOLEDs with the emitting layer prepared by solution-processing recently, wherein the emitters are very often mixed with a soluble host and suitable phosphor in the past several years.

Carbazole derivatives are generally used as the host in PhOLEDs for their relatively high triplet energy and moderate hole-transport ability. Among them, 4,4'-*N*,*N*-dicarbazolebiphenyl (CBP) is representative host material for electrophosphorescent devices.[11] However, CBP is far from an ideal host. It has a distinct T_c of 199 ℃, which indicates its crystallization nature.

To improve the device performance, new small-molecule hosts were design for solution-processed PhOLEDs. First of all, to improve thermal stability and electron injection, cyclohexanyl or adamatyl groups between two phenyl rings of CBP were introduced (Cy-Cz, Ad-Cz).[12]

Of the few highly efficient solution-processed OLEDs reported, most devices were investigated with one or more thermal evaporation layers to achieve better balance of charge transport. On the other hand, to balance the charge recombination efficiency, one promising strategy is to mix the hole- and electron-transporting host materials.[13] As expected, good performance which was comparable with that of the similar vacuum deposited OLEDs, may be due to the appropriate combination of host molecules with proper energy levels, mobilities, and film forming properties.

For efficient solution-processed blue POLEDs, a high triplet energy gap (>2.7 eV) is necessary, which prevents the reverse energy transfer from the dopant to the host. To satisfy requirements, carbazole and/or fluorene moieties were introduced (TBCPF, BTCC-27, BTCC-36, SimCP).[14]

Bipolar molecules bearing both electron and hole transporting moieties have attracted considerable interest because their ability to transfer holes and electrons simultaneously. The simplified devices with double-layer or even single-layer structure could be thereby attained based on bipolar materials. By combining suitable electron-rich and -deficient moieties into a molecular structure, several solution-processed bipolar host materials have been synthesized (TBBI, Me-TBBI, TIBN, Me-TIBN, DM-TIBN, tBu-OXDTFA, CzOXD).[15]

I-4. References

1. N. J. Turro, V. Ramamurthy and J. C. Scaiano, *Principles of Molecular Photochemistry : An Introduction*, University Science Books : Sausalito, California, Chapter 2 (2008)
2. B. G. Streetman and S. K. Banerjee, *Solid State Electronic Devices*, Pearson Education, Upper Saddle River, New Jersey, Chapter 5 (2006)
3. J. G. Simmons, *J. Phys. D*, 1971, **4**, 613.
4. N. F. Mott and E. A. Davis, *Electronic in Non-Crystalline Materials*, Oxford Univ. Press, Oxford (1979)
5. N. J. Turro, V. Ramamurthy and J. C. Scaiano, *Principles of Molecular Photochemistry : An Introduction*, University Science Books : Sausalito, California, Chapter 7 (2008)
6. J. Kido, M. Kohda, K. Okuyama and K. Nagai, *Appl. Phys. Lett.* 1992, **61**, 761.
7. J. Kido, K. Hongawa, K. Okuyama and K. Nagai, *Appl. Phys. Lett.* 1993, **63**, 2627.
8. (a) M. Gross, D. C. Nuller, H. -G. Nothofer, U. Scherf, D. Neher, C. Brauchle and K. Meerholz, *Nature*, 2000, **405**, 661; (b) X. Chen, J. -L. Liao, Y. Liang, M. O. Ahmed, H. -E. Tseng and S. -C. Chen, *J. Am. Chem. Soc.* 2003, **125**, 636; (c) R. W. T. Higgins, A. P. Monkman, H. -G. Nothofer and U. Scherf, *J. Appl. Phys.* 2002, **91**, 99; (d) W. Zhu, C. Liu, L. Su, W. Yang, M. Yuan and Y. Cao, *J. Mater. Chem.* 2003, **13**, 50; (e) F. -C. Chen, Y. Yang, M. E. Thompson and J. Kido, *Appl. Phys. Lett.* 2002, **80**, 2308.
9. A. van Dijken, J. J. A. M. Bastiaansen, N. M. M. Kiggen, B. M. W. Langeveld,

C. Rothe, A. Monkman, I. Bach, P. Stossel, and K. Brunner, *J. Am. Chem. Soc.* 2004, **126**, 7718.

10. X. H. Yang, D. Neher, D. Hertel and T. K. Daubler, *Adv. Mater.* 2004, 16, 161.
11. C. Adachi, M. A. Baldo, M. E. Thompson and S. R. Forrest, *J. Appl. Phys.*, 2001, **90**, 5048.
12. K. Watanabe, D. Kumaki, T. Tsuzuki, E. Tokunaga and S. Tokito, *J. Photopolym. Sci. Technol.* 2007, **20**, 39.
13. (a) H. Kim, Y. Byun, R. R. Das, B. K. Choi and P. S. Ahn, *Appl. Phys. Lett.* 2007, **91**, 093512; (b) Y. Hino, H. Kajii and Y. Ohmori, *Org. Electron.* 2004, **5**, 265; (c) Y. Hino, H. Kajii and Y. Ohmori, *Jpn. J. Appl. Phys.* 2005, **44**, 2790; (d) J. -H. Jou, M. -C. Sun, H. -H. Chou and C. -H. Li, *Appl. Phys. Lett.* 2006, **88**, 141101.
14. (a) L. D. Hou, L. Duan, J. Qiao, W. Li, D. Q. Zhang and Y. Qiu, *Appl. Phys. Lett.* 2008, **92**, 263301; (b) W. Jiang, L. Duan, J. Qiao, G. Dong, D. Zhang, L. Wang and Y. Qiu, *J. Mater. Chem.* 2011, **21**, 4918; (c) M. F. Wu, S. J. Yeh, C. T. Chen, H. Murayama, T. Tsuboi, W. S. Li, I. Chao, S. W. Liu and J. K. Wang, *Adv. Funct. Mater.* 2007, **17**, 1887.
15. (a) Z. Ge, T. Hayakawa, S. Ando, M. Ueda, T. Akiike, H. Miyarnoto, T. Kajita and M. A. Kakimoto, *Chem. Mater.* 2008, **20**, 2532; (b) Z. Y. Ge, T. Hayakawa, S. Ando, M. Ueda, T. Akiike, H. Miyamoto, T. Kajita and M. A. Kakimoto, *Adv. Funct. Mater.* 2008, **18**, 584; (c) C. H. Chien, L. R. Kung, C. H. Wu, C. F. Shu, S. Y. Chang and Y. Chi, *J. Mater. Chem.* 2008, **18**, 3461; (d) Y. T. Tao, Q. Wang, C. L. Yang, K. Zhang, Q. Wang, T. T. Zou, J. G. Qin and D. G. Ma, *J. Mater. Chem.* 2008, **18**, 4091.

Chapter II. Tetraphenylsilane Containing Solution-Processable Small-Molecular Hosts for Highly Efficient Phosphorescent Organic Light-Emitting Diodes

II-1. Introduction

Since the first organic light-emitting diodes (OLEDs) were reported in 1987 by Tang and Van Slyke,[1] many efforts have been made to develop OLEDs and significant progress has been made in the various applications.[2] OLEDs have many advantages for display and lighting application such as wide viewing angle, fast response and light weight, etc.[3] Especially, phosphorescent organic light-emitting diodes (PhOLEDs) showed a high efficiency because phosphorescent emitter containing transition metals (Ir(III), Pt(II) etc.) that enable to harvest both singlet and triplet exitons, thus provide 100% internal quantum efficiency for light emission.[4] Up to date, efficient PhOLEDs were fabricated through the vacuum vapor deposition[5] which include complex processes and waste many organic materials, thus lead high costs. Hence, the application to roll-to-roll processed devices, large-area devices is difficult to realize. Therefore, for low cost and easy fabrication, solution-processed device is desirable.[6] Even though polymer light-emitting diodes (PLEDs) can be easily fabricated by solution-process, polymers are generally difficult to synthesize and purify, and they have dispersed molecular

weights for electronic devices.[7] In these regards, developing low-molecular-weight (small-molecular) host materials suitable for solution-process will possess both advantages of high-efficiency known from small-molecule-based devices and easy-fabrication known from polymer-based devices. In the most PhOLEDs, besides, host-dopant system is adopted as an emission mechanism, owing to reducing competitive factors such as concentration quenching and triplet-triplet annihilation of phosphorescent emitters.[8] Therefore, choosing appropriate host material for PhOLEDs is critical to determine device performances.[9] But common small-molecular host materials tend to recrystallize because of less amorphous structure, poor solubility for common organic solvents.[10] To acquire high-quality films, small-molecular host materials must possess amorphous character. They also must possess thermal and electrochemical stabilities for stable device operation. These factors play a significant role to determine device performances. To satisfy these requirements, (i) carbazole-based host materials,[11] (ii) arylsilane-based host materials,[12] (iii) tripheynlamine-based host materials,[13] (iv) phosphine-oxide-based host materials[14] have been reported in PhOLEDs. Among these, carbazole-based host materials are most widely used as host materials, owing to their high triplet energy, excellent hole transporting properties.[11] However, as previously stated, co-planar structure of carbazole tends to recrystallize[10] and form excimer upon device fabricating,[11h,15] which results in detrimental influence such as limiting device efficiency and forming charge trapping sites.[11h] Herein, new solution-processable small-molecular host materials (TPS series) comprising both carbazole group and tetraphenylsilane (TPS) group (Scheme 1) were reported. TPS group effectively prevents intermolecular interactions between adjacent carbazoles, thus suppress

excimer formation of TPS series. TPS group also makes TPS series to form amorphous structure through highly twisted, bulky character. Additionally, TPS group induces improvement of thermal and morphological stabilities of TPS series. Therefore, it was proved that TPS series are suitable to solution-processed devices in this work. For example, TPS_4DCz was synthesized from 1,2-*trans*-di(carbazol-9-yl)cyclobutane (DCz)[11h] which was good at blue electrophosphorescent devices as a host material with high triplet level. By attaching TPS group to DCz, solution-processability, amorphous character, and high thermal/electrochemical stabilities were achieved to TPS_4DCz. Poly-(*N*-vinylcarbazole) (PVK), which is most widely used for PhOLEDs as a host material and has carbazole group that comparable to TPS series, was used for control material to TPS series. TPS series showed much better properties as a host material than PVK and TPS series-based devices showed superior performances to PVK-based devices. As the number of TPS group increases, furthermore, this phenomenon was intensified. In this paper, the influences of TPS group attached to carbazole group will be shown.

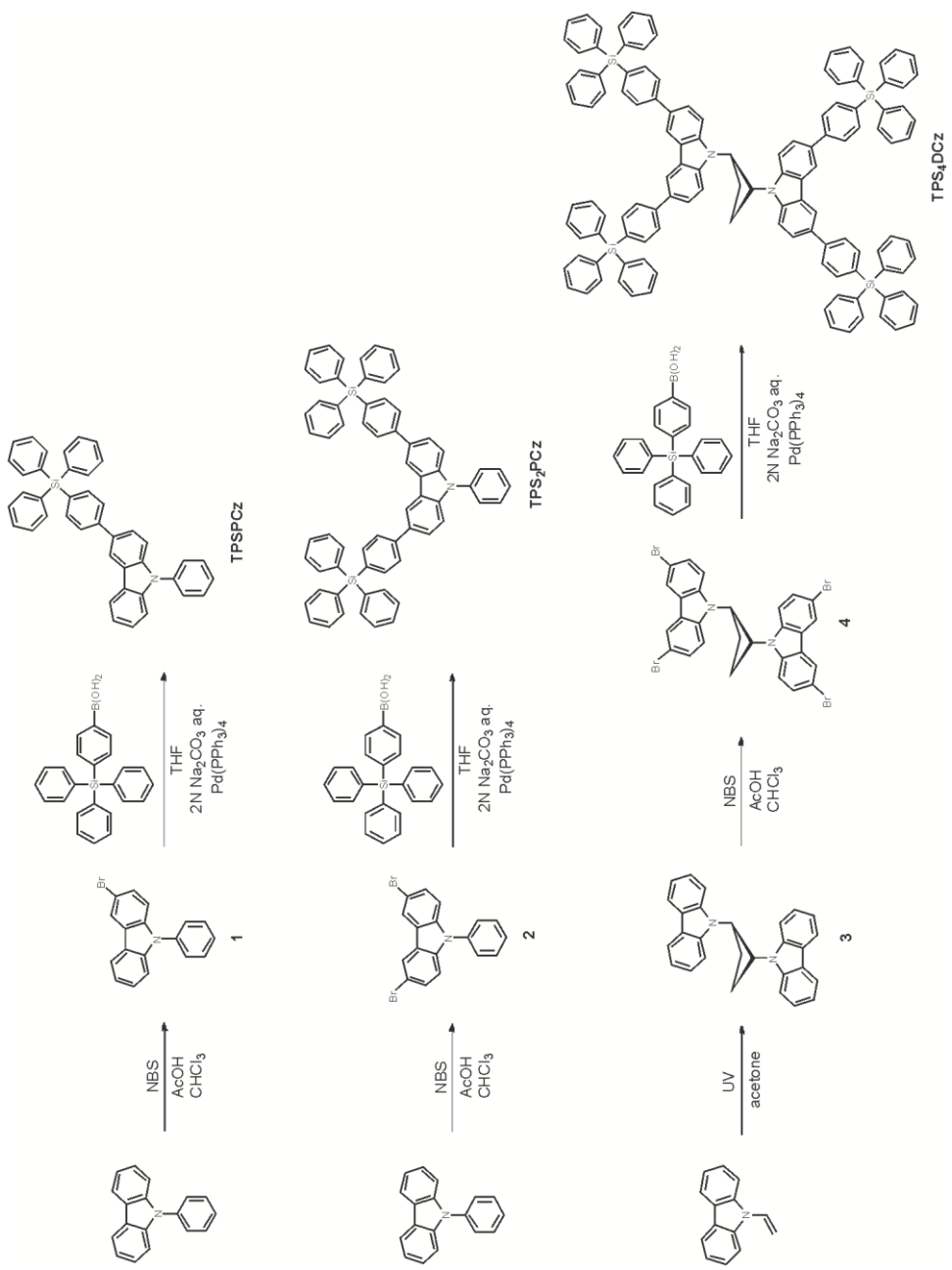

Scheme 1 Synthetic routes of TPSPCz, TPS_2PCz and TPS_4DCz.

II-2. Results and Discussion

II-2-1. Syntheses

Scheme 1 illustrates the synthetic routes and molecular structures of TPSPCz, TPS_2PCz and TPS_4DCz. First of all, 1,2-*trans*-di(carbazol-9-yl)cyclobutane (**2**) was synthesized by previous method.[11h] 3-bromo-9-phenyl-carbazole, 3,6-dibromo-9-phenyl-carbazole (**1**) and 1,2-bis(3,6-dibromo-carbazol-9-yl)cyclobutane (**3**) were synthesized by bromination reaction with *N*-bromosuccinimide (NBS) in acetic acid and chloroform. TPSPCz, TPS_2PCz and TPS_4DCz were synthesized by Suzuki-Miyaura coupling reaction with (4-(triphenylsilyl)phenyl)boronic acid in the presence of tetrakis(triphenylphosphine) palladium ($Pd(PPh_3)_4$), tetrahydrofuran (THF), 2N Na_2CO_3 aqueous solution. The precursors are assigned and characterized by ^{1}H NMR. The final products are assigned and characterized by ^{1}H and ^{13}C NMR, elemental analysis, mass spectrometry (see Experimental section for details).

II-2-2. Photophysical Properties

Figure 1 shows room-temperature absorption and photoluminescence (PL) spectra of the compounds in dichloromethane (DCM) (10 μM) and also the spectra of pristine and $Ir(PPy)_3$ doped spin-coated films. The photophysical properties are also summarized in Table 1. It is obvious that the photophysical characteristics of neat films or solutions are nearly identical with TPS series each other and thus can be certainly attributed to the lowest π-π* transition of the central carbazole core. Thus the TPS group serves as effective spacers, blocking the π-conjugation of the carbazole core extending to the adjacent TPS or phenyl groups.

Full-width at half maximum (FWHM) values and bathochromic shift of neat film emission peak are shown in Table 1. The bathochromic shift, which is from solution to thin film, of emission peak of TPS series (4 nm for TPSPCz, 8 nm for TPS_2PCz and 4 nm for TPS_4DCz) is much shorter than that of PVK (36 nm). The FWHM values of all TPS series (44 nm for TPSPCz, 52 nm for TPS_2PCz and 41 nm for TPS_4DCz) are smaller than that of PVK (74 nm). These facts indicate that excimer formation between adjacent carbazole units was effectively suppressed in TPS series through site-isolation effect of TPS group. That is, intermolecular interactions are effectively suppressed by introduction of bulky TPS group.

Absorption spectrum of $Ir(PPy)_3$ overlapped well with emission spectrum of host materials. Therefore, it was expected that TPS series are suitable as host materials for $Ir(PPy)_3$ as an emitter and effective Förster energy transfer. It was proved that emission of $Ir(PPy)_3$ is dominant in PL spectrum of $Ir(PPy)_3$ doped films (as shown

in Figure 1).

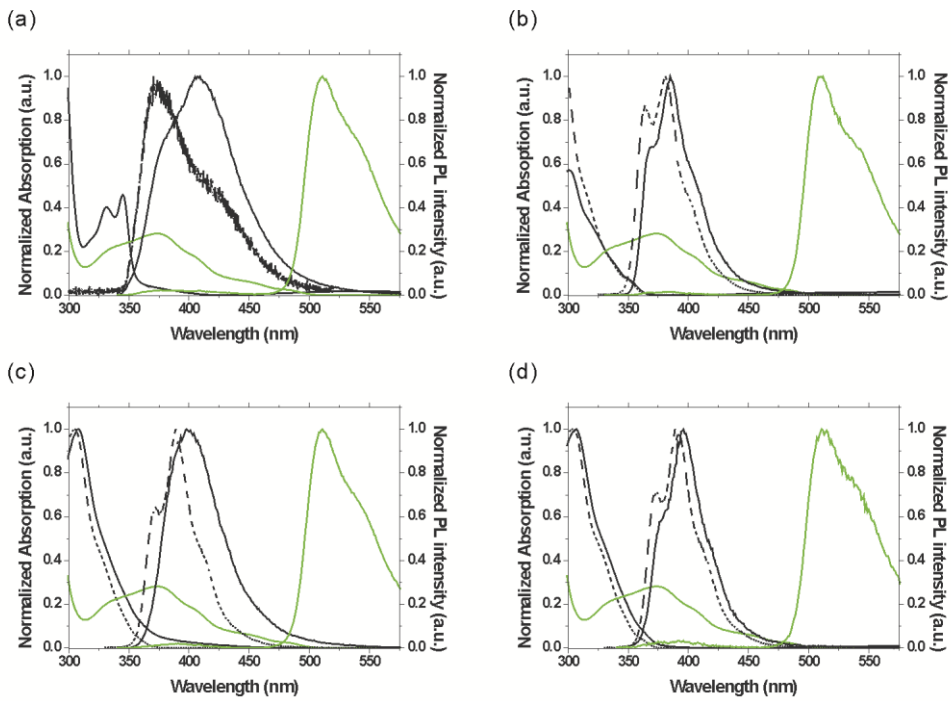

Figure 1 Normalized absorption and PL spectra of (a) PVK, (b) TPSPCz, (c) TPS_2PCz and (d) TPS_4DCz (UV-vis : dashed - sol'n; solid - film; green - $Ir(PPy)_3$ only, PL : dashed - sol'n; solid - film; green - $Ir(PPy)_3$ doped film).

Table 1 Physical data of TPS series

Compound	$T_g/T_{d,5\%}$ (°C)	λ_{abs} [a,b] (nm)	$\lambda_{em,\ max}$ [a,b] (nm)	$\Delta\lambda_{em,\ max}$ [c] (nm)	$FWHM_{em}$ [a] (nm)	HOMO/LUMO [d,e] (eV)
TPSPCz	- [f]/363	297	385	4	44	5.83/2.22
		(298)	(381)			(5.44/1.01)
TPS2PCz	162/424	308	398	8	52	5.91/2.43
		(305)	(390)			(5.40/1.08)
TPS4DCz	- [f]/471	307	396	4	41	5.88/2.40
		(304)	(392)			(5.22/0.95)

[a] measured in neat film; [b] measured in DCM and a concentration of 10 μM (in the parenthesis); [c] from solution to thin film; [d] values from experiment (AC-2, optical band-gap); [e] values from DFT calculation (in the parenthesis); [f] not detected upon heating the sample up to 300°C.

II-2-3. Theoretical Calculations

To discover the structure-characteristic relationship of the compounds at the molecular level, the geometrical and electronic properties of the compounds were studied using density functional theory (DFT) calculations. The geometry of three compounds were optimized by using Gaussian 09 at the B3LYP/6-31G(d,p) level in *vacuo* condition.[16]

The optimized geometries of the compounds are shown in Figure 2. The TPS group and phenyl group of the compounds are significantly twisted with the carbazole core, resulting in a non-coplanar structure. These twisted structures effectively prevent intermolecular interactions, thus suppress their recrystallization and limit the extent of conjugation length, which improves the morphological stability of thin films. TPS_4DCz showed especially significant twisted structure, which is caused by 1,2-*trans* configuration of DCz along cyclobutane. As shown in Figure 2, dihedral angle of two carbazole groups in TPS_4DCz is about 90°. This result indicates that intermolecular interaction between π-systems of two carbazole groups in TPS_4DCz is well suppressed.

As increasing number of TPS groups, phenyl groups attached to C3, C6-position of carbazole core are less and less involved in formation of energy gap (Figure 2). This observed result is caused by the highly twisted structure of TPS series, which interrupt π-conjugation from carbazole core to TPS group. In other words, TPS groups appear to have little effect on wide band-gap characteristic of carbazole. It was also noticed that LUMO/LUMO+1 of TPS_4DCz are localized at each

carbazole, respectively, and similar in energy levels. The calculated energy-gap values of the compounds are 4.43 eV for TPSPCz, 4.32 eV for TPS_2PCz, 4.27 eV for TPS_4DCz (calculated HOMO/LUMO values are shown in Table 1).

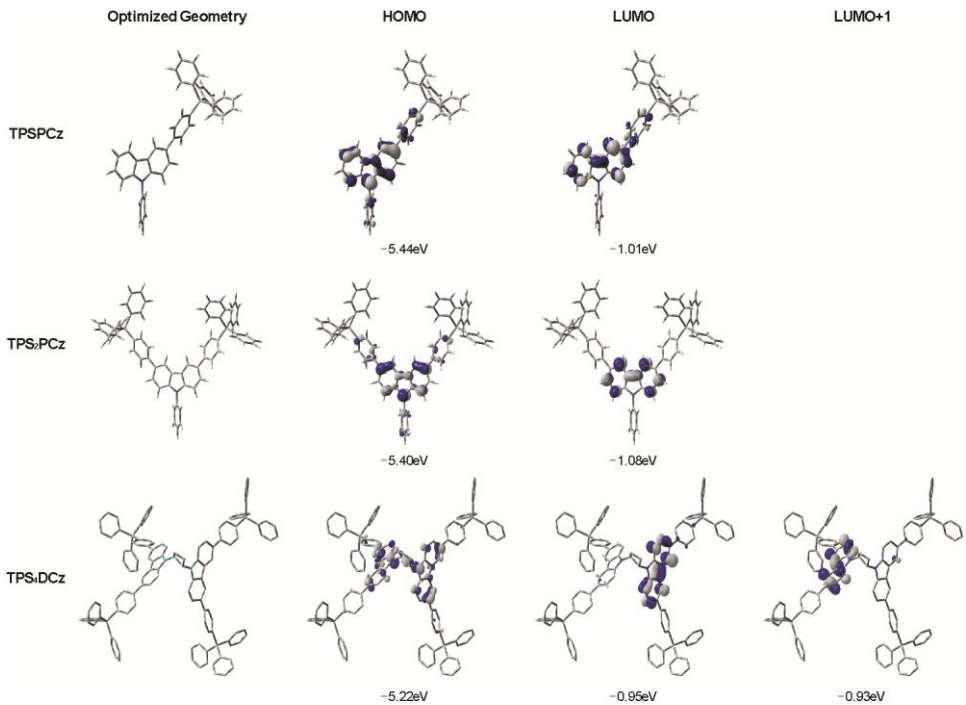

Figure 2 Three-dimensional optimized geometry, calculated HOMO/LUMO/LUMO+1 electron density map and orbital energies of TPS series by DFT calculation (for legibility, hydrogens of TPS_4DCz were hided).

II-2-4. Thermal Properties

The thermal properties of the compounds were investigated by thermogravimetric analysis (TGA) and differential scanning calorimetry (DSC) (Figure 3), and summarized in Table 1. The three compounds exhibit high thermal decomposition temperatures ($T_{d,5\%}$, corresponding to 5% weight loss) and the $T_{d,5\%}$ of TPSPCz, TPS_2PCz and TPS_4DCz are 363 ℃, 424 ℃ and 472 ℃, respectively. They also exhibit high glass-transition temperatures (T_g). Especially, TPS_4DCz exhibits extremely high thermal stability (T_g of TPS_4DCz was not detected upon heating the sample up to 300 ℃), which is among the highest T_g reported for host materials. This undetected T_g means that TPS_4DCz has fully amorphous structure. And these thermal properties of the compounds are much better than another carbazole-based and arylsilane-based host materials.[11-12] These facts indicate that the introduction of TPS group significantly improves thermal stability. And the excellent thermal stability with high T_g and $T_{d,5\%}$ values should improve the morphological stability of the film and reduce the possibility of phase separation upon device fabricating and operating.[17] Therefore, the compounds are more promising in terms of its thermal properties for application in OLEDs devices. Besides, their thermal stabilities tend to determine depending on the number of TPS group.

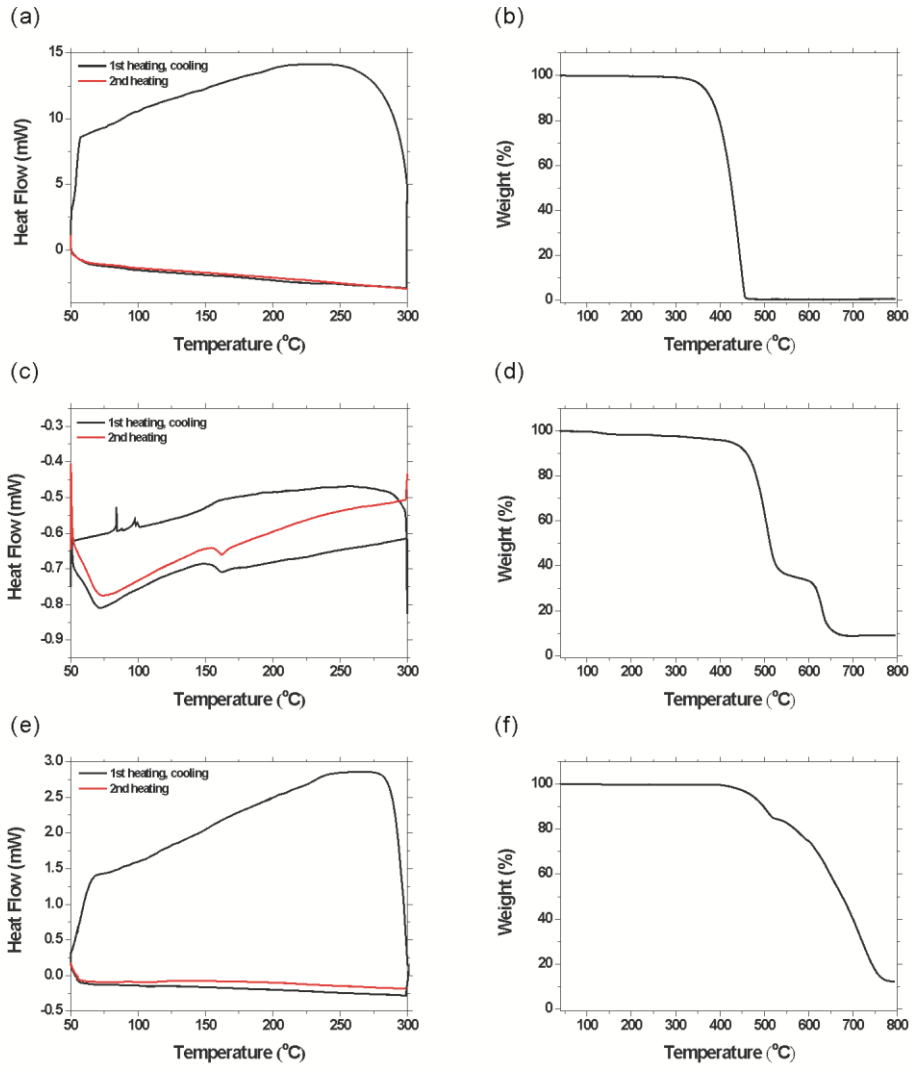

Figure 3 DSC traces of (a) TPSPCz, (c) TPS_2PCz, (e) TPS_4DCz recorded at a scan rate of 10 °C min^{-1} and TGA traces of (b) TPSPCz, (d) TPS_2PCz, (f) TPS_4DCz recorded at a scan rate of 10 °C min^{-1}.

II-2-5. Morphological Studies

Atomic force microscopy (AFM) was used to investigate morphologies of thin films. The films were prepared through spin-coating from a chlorobenzene solution onto pre-cleaned glass substrates and then heated at 100 ℃ for 30 min to remove the residue solvent under nitrogen atmosphere. According to images of Figure 4, the surfaces of neat TPS series films are free of pinholes and quite smooth, and the root-mean-square (RMS) values of TPSPCz, TPS_2PCz and TPS_4DCz are 0.429, 0.517 and 0.192 nm, respectively. The films doped with 8 wt% $Ir(PPy)_3$ are also measured, RMS values are 0.246, 0.473 and 0.340 nm respectively, and no phase-separation is detected. These results are highly important in improving the efficiency and lifetime of PhOLEDs. However, the films prepared from PVK doped with Ir(III) complexes exhibited RMS value of 8.247 nm, and a kind of phase-separation or aggregations. These results indicate that TPS series have good miscibility with Ir(III) complexes[18] and are capable of forming solution-processed amorphous films through site-isolation effect of bulky TPS group.

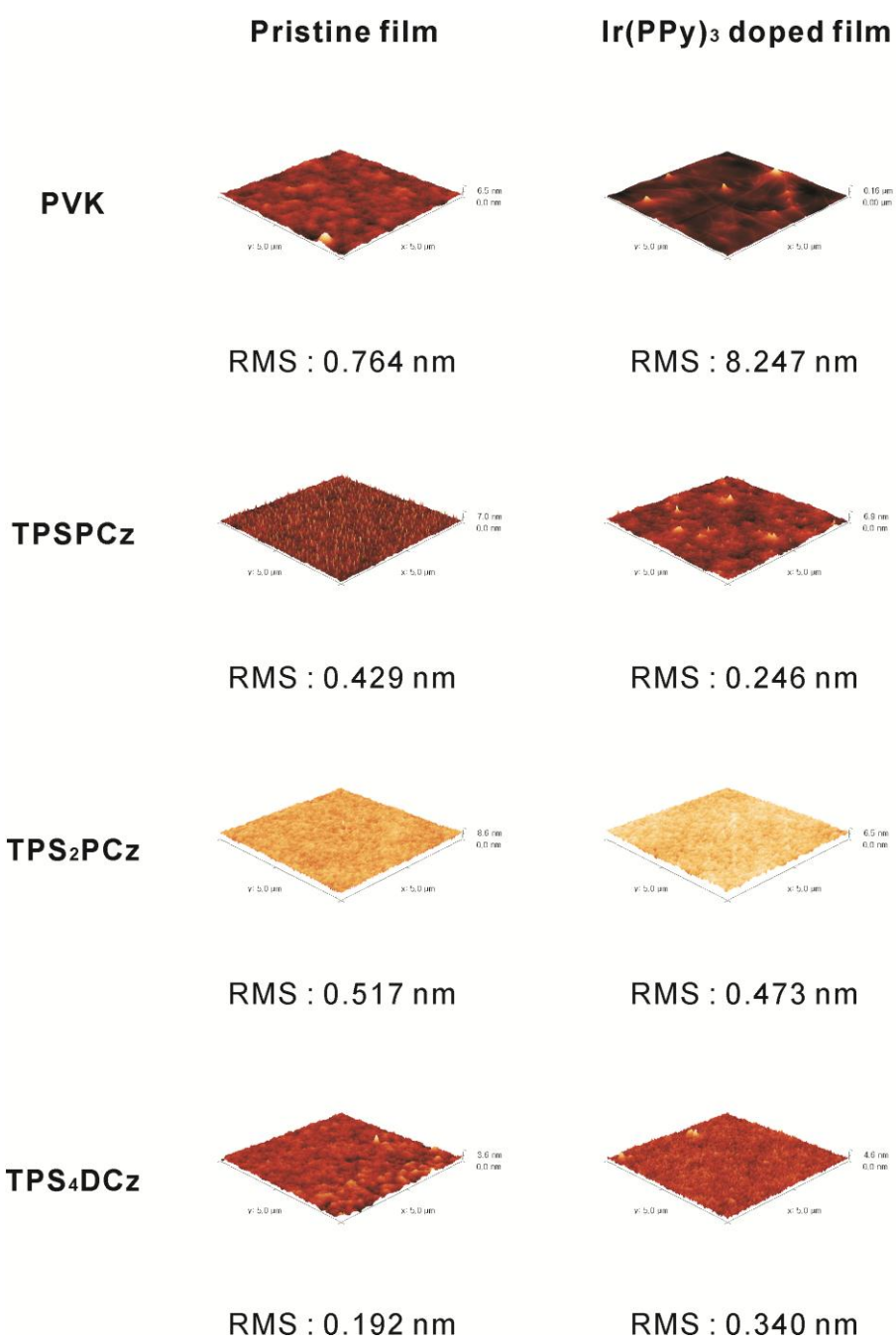

Figure 4 AFM topographic images and rms values of PVK and TPS series.

II-2-6. Electrochemical Properties

The electrochemical properties of the compounds were studied by using cyclic voltammetry (CV) analyses in solution state (Figure 5). During repeated scans in dichloromethane, all TPS series showed same reversible oxidation behaviors, respectively (Figure 5). Such characteristics are attributed to the introduction of TPS group at the active site of carbazole (C3, C6-positions) which means protecting active sites of carbazole enhances electrochemical stability of the compounds. This is an important factor in case of the compounds have charge carrier characteristic in OLEDs.[19] In contrast, active sites of carbazole are left unprotected as PVK, the oxidation process was not reversible, with the oxidation potential gradually shifting to lower potentials and the current increasing during repeated CV scans (Figure 5(a)). Such characteristics are signatures of electrochemical polymerization of carbazoles, which lower device performance, through the active C3 and C6 sites of carbazole.[20]

The HOMO level was observed at -5.83, -5.91 and -5.88 eV of TPSPCZ, TPS_2PCz and TPS_4DCz by atmospheric photoelectron spectroscopy (AC-2). The LUMO energy was calculated at -2.22, -2.43 and -2.40 eV of TPSPCz, TPS_2PCz and TPS_4DCz by adding of the optical energy gap (E_g) from the HOMO level. These observed energy levels are more suitable for effective charge injection from another layer of device than calculated energy levels.

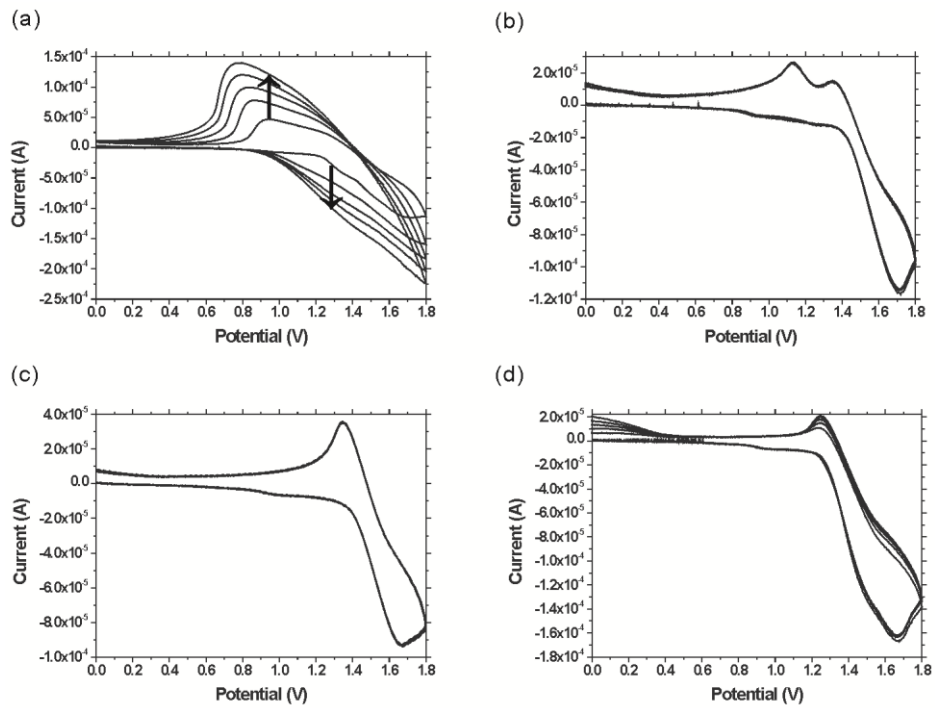

Figure 5 Oxidation part of CV curves of (a) PVK, (b) TPSPCz, (c) TPS_2PCz and (d) TPS_4DCz in dichlromethane solution (5-cycles scan).

II-2-7. Electroluminescent Properties

The solution-processed green electrophosphorescent OLEDs have been fabricated using $Ir(PPy)_3$ as an emitter with an optimized concentration of 8 wt%, the device have a configuration of ITO/PEDOT:PSS (40 nm)/host : $Ir(PPy)_3$ (8 wt%, 30 nm)/2,9-dimethyl-4,7-diphenyl-1,10-phenanthroline (BCP) (20 nm)/tris(8-hydroxy-quinolinato) aluminium (Alq_3) (30 nm)/ LiF (1 nm)/Al (100 nm). PEDOT:PSS and LiF are used as hole- and electron-injection materials, respectively. BCP and Alq_3 are used as electron-transporting materials. The relative energy levels of the materials used for the devices are shown in Figure 6(a). And Figure 6(c), Figure 6(d) show the current density–voltage–brightness (*J–V–L*) characteristics and external quantum efficiency versus current density curves for the devices, and the EL data are summarized in Table 2. TPSPCz:$Ir(PPy)_3$ device showed a maximum current efficiency ($\eta_{c,\,max}$) of 20.24 cd A^{-1}, a maximum power efficiency ($\eta_{p,\,max}$) of 9.79 lm W^{-1}, a maximum external quantum efficiency ($\eta_{ext,\,max}$) of 7.47 %. TPS_2PCz:$Ir(PPy)_3$ device showed a maximum current efficiency ($\eta_{c,\,max}$) of 23.67 cd A^{-1}, a maximum power efficiency ($\eta_{p,\,max}$) of 13.14 lm W^{-1}, a maximum external quantum efficiency ($\eta_{ext,\,max}$) of 7.60 %. TPS_4DCz:$Ir(PPy)_3$ device showed a maximum current efficiency ($\eta_{c,\,max}$) of 25.10 cd A^{-1}, a maximum power efficiency ($\eta_{p,\,max}$) of 10.70 lm W^{-1}, a maximum external quantum efficiency ($\eta_{ext,\,max}$) of 8.95 %. These values are much superior to those of the PVK:$Ir(PPy)_3$ device, which showed a maximum current efficiency ($\eta_{c,\,max}$) of 16.51 cd A^{-1}, a maximum power efficiency ($\eta_{p,\,max}$) of 5.60 lm W^{-1}, a maximum external quantum efficiency

($\eta_{ext,\ max}$) of 3.52 %.

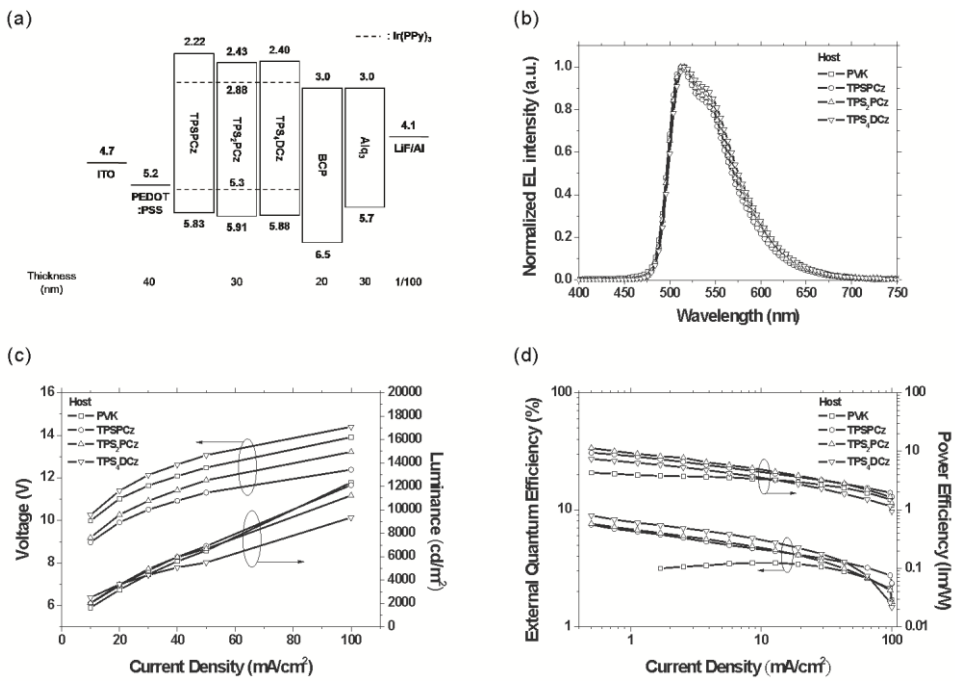

Figure 6 (a) Energy level diagram, (b) EL spectra at 10 mA cm^{-2} (c) *J-V-L* characteristics, (d) External quantum efficiency and power efficiency versus current density curves for TPS-series:$Ir(PPy)_3$ devices.

Table 2 Electroluminescence properties of the devices.[a]

Device	V_{on} (V)	η_c [b] (cd A^{-1})	η_p [b] (lm W^{-1})	η_{ext} [b] (%)	CIE[c] (x,y)
PVK:Ir(PPy)$_3$	4.60	16.51	5.60	3.52	(0.317,0.607)
		16.51	5.20	3.52	
TPSPCz:Ir(PPy)$_3$	4.80	20.24	9.79	7.47	(0.305,0.624)
		20.24	7.08	4.42	
TPS_2PCz:Ir(PPy)$_3$	4.80	23.67	13.14	7.60	(0.311,0.622)
		20.62	7.05	4.52	
TPS_4DCz:Ir(PPy)$_3$	4.80	25.10	10.70	8.95	(0.325,0.616)
		25.10	7.69	5.25	

[a] abbreviations : V_{on} : turn-on voltage, η_c : current efficiency, η_p : power efficiency, η_{ext} : external quantum efficiency, CIE (x, y) : Commission International de I'Eclairage coordinates; [b] order of measured value : maximum, then values at 10 mA cm^{-2}; [c] measured at 10 mA cm^{-2}.

Especially, TPS_4DCz:$Ir(PPy)_3$ device showed much higher maximum external quantum efficiency than PVK:$Ir(PPy)_3$ device by 154 times. These performances of TPS series:$Ir(PPy)_3$ devices are highly outstanding with respect to previously reported works based on solution-processed green electrophosphorescent devices using $Ir(PPy)_3$ as an emitter.[21] This result is consistent with the view that the introduction of TPS groups into the carbazole can reduce the intermolecular interactions and suppress triplet–triplet annihilation of organometallic compounds in the devices.[8,18]

Electroluminescence (EL) spectra are shown in Figure 6(b). Completely no emission coming from the TPS series and pure emission from $Ir(PPy)_3$ were observed as shown in Figure 6(b), indicative of efficient energy transfer from the TPS series to $Ir(PPy)_3$.

To further evaluate the suitability of the compounds as host materials for blue and red phosphorescent emitters, TPS_4DCz:FIrpic, TPS_4DCz:$Ir(Piq)_2acac$ devices were fabricated by using TPS_4DCz as the host, 8 wt% iridium (III) bis [(4,6-difluorophenyl)-pyridinato-*N*,$C^{2'}$] picolinate (FIrpic) and bis (1-(phenyl)-isoquinoline) iridium (III) acetylacetonate [$Ir(Piq)_2acac$] as the dopants, respectively. TPS_4DCz:FIrpic and TPS_4DCz:$Ir(Piq)_2acac$ devices are comprised of the same configuration with green electrophosphorescent device. TPS_4DCz is chosen for the blue and red electrophosphorescent device test on the basis of the best performance on the green electrophosphorescent device. And Figure 7 shows the current density–voltage–brightness (*J*–*V*–*L*) characteristics and external quantum efficiency versus current density curves for the devices, and the EL data are summarized in Table 3. The device TPS_4DCz:FIrpic showed a current

efficiency ($\eta_{c,\ max}$) of 5.57 cd A^{-1}, a power efficiency ($\eta_{p,\ max}$) of 2.13 lm W^{-1}, a external quantum efficiency ($\eta_{ext,\ max}$) of 3.37 %. The device TPS_4DCz:$Ir(Piq)_2acac$ showed a current efficiency ($\eta_{c,\ max}$) of 2.33 cd A^{-1}, a power efficiency ($\eta_{p,\ max}$) of 1.11 lm W^{-1}, an external quantum efficiency ($\eta_{ext,\ max}$) of 4.22 %. The device PVK:FIrpic showed a current efficiency ($\eta_{c,\ max}$) of 6.81 cd A^{-1}, a power efficiency ($\eta_{p,\ max}$) of 2.37 lm W^{-1}, an external quantum efficiency ($\eta_{ext,\ max}$) of 2.62 %. The device PVK: $Ir(Piq)_2acac$ showed a current efficiency ($\eta_{c,\ max}$) of 2.27 cd A^{-1}, a power efficiency ($\eta_{p,\ max}$) of 0.88 lm W^{-1}, a external quantum efficiency ($\eta_{ext,\ max}$) of 3.54 %. The performances of devices TPS_4DCz:FIrpic and TPS_4DCz:$Ir(Piq)_2acac$ are comparable to those of the PVK-based devices, respectively.

These all results indicate that TPS series enables organometallic compounds to be solution-processed by mixing TPS series and organometallic compounds, which cannot be solution-processed alone. And the results indicate also that TPS series host materials are universal host materials for RGB phosphors.

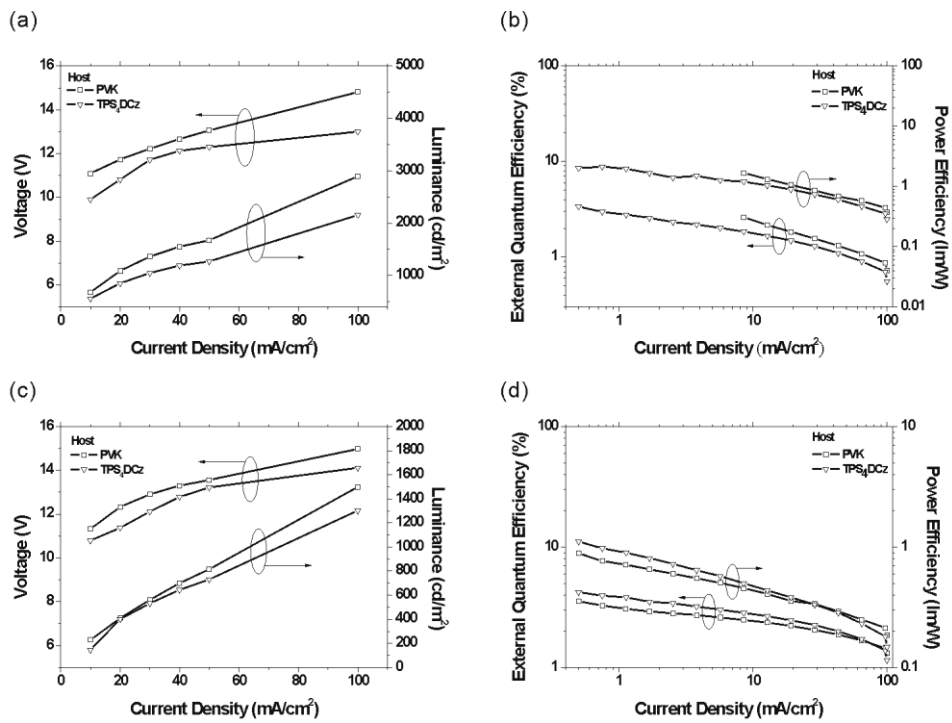

Figure 7 *J-V-L* characteristics of (a) TPS_4DCz:FIrpic device, (c) TPS_4DCz:$Ir(Piq)_2acac$ device and external quantum efficiency and power efficiency versus current density curves for (b) TPS_4DCz:FIrpic device, (d) TPS_4DCz:$Ir(Piq)_2acac$ device.

Table 3 Electroluminescence properties of the blue and red devices.[a]

Device	V_{on} (V)	η_c [b] (cd A^{-1})	η_p [b] (lm W^{-1})	η_{ext} [b] (%)	CIE[c] (x,y)
PVK:FIrPic	6.80	6.81	2.37	4.22	(0.181,0.371)
		6.81	1.93	2.16	
TPS_4DCz:FIrpic	6.20	5.57	2.13	3.37	(0.183,0.375)
		5.57	1.77	1.67	
PVK:$Ir(Piq)_2acac$	6.40	2.27	0.88	3.54	(0.660,0.317)
		2.27	0.63	2.36	
TPS_4DCz:$Ir(Piq)_2acac$	7.40	2.33	1.11	4.22	(0.677,0.320)
		2.33	0.71	2.67	

[a] abbreviations : V_{on} : turn-on voltage, η_c : current efficiency, η_p : power efficiency, η_{ext} : external quantum efficiency, CIE (x, y) : Commission International de l'Eclairage coordinates; [b] order of measured value : maximum, then values at 10 mA cm^{-2}; [c] measured at 10 mA cm^{-2}

II-3. Conclusion

In summary, a new series of solution-processable small-molecular host materials for PhOLEDs has been developed. The compounds are comprised of carbazole core and tetraphenylsilane (TPS) groups. The compounds showed extremely high thermal and electrochemical stabilities, and showed significantly twisted structures, which prevent recrystallization and suppress formation of eximers between adjacent carbazole groups, enhanced film formability, amorphous/solution-processable nature through site-isolation effect. Highly efficient green solution-processed electrophosphorescent devices have been successfully reallized by using TPS series as host materials. Especially, the device TPS_4DCz:$Ir(PPy)_3$ device showed excellent maximum external quantum efficiency of 8.95 %. The performances of the TPS series-based devices are far superior to those of the corresponding PVK-based devices. Through these results, it was confirmed that the enhanced device performances and properties have achieved by introduction of TPS groups. And TPS series host materials can be used as universal host materials for RGB phosphors, and finally will be able to realize for single emitting layer white PhOLEDs. Also, such findings as cost-effective solution-processed PhOLEDs shall provide useful guidelines for the future display and lighting applications.

II-4. Experimental

II-4-1. General Information

All materials were obtained from commercial suppliers and used without further purification. ^{1}H NMR and ^{13}C NMR measurements were carried out on a Bruker Avance-300 and Bruker Avance-500 NMR spectrometer, respectively. GC-MS was carried out with JEOL JMS-700, matrix-assisted laser desorption ionization time-of-flight (MALDI-TOF) was carried out with Voyager-DE^{TM} STR Biospectrometry Workstation. Elemental analyses were carried out on a CE Instrument EA1112. Thermogravimetric analysis (TGA) was carried out using a TA instruments Q50 model under a dry nitrogen gas flow at a heating rate of 10 ℃ min^{-1}. T_g (the glass transition temperature) are determined by differential scanning calorimetry (DSC) at a heating rate of 10 ℃ min^{-1} using a TA Instrument DSC-Q1000. The absorption and photoluminescence spectra were measured with a UV-visible spectrophotometer (SHIMADZU UV-1650PC) and a fluorospectrophotometer (Varian Cary Eclipse fluorescence spectrophotometer), respectively. The cyclic voltammetric measurements were performed using a 273A (Princeton Applied Research) with a one-compartment electrolysis cell consisting of a Pt working electrode, a quasi Ag^{+}/Ag reference-electrode and a Pt-wire counter-electrode. The supporting electrolyte was 0.1 M tetrabutylammonium tetrafluoroborate in CH_2Cl_2 (0.5 mM), and the electrochemical measurements were carried out at a scan rate of 100 mV s^{-1}, with ferrocene as internal reference. The film surface morphology was

measured with atomic force microscopy (AFM, PSIA XE-100). All the measurements were carried out in air at room temperature without further encapsulation.

II-4-2. Materials

9-phenyl-3-(4-(triphenylsilyl)phenyl)-carbazole (TPSPCz) : A 9-phenyl-carbazole (4.11 mmol, 1 g) was dissolved in 100 mL of acetic acid and 120 mL of chloroform. *N*-bromosuccinimide (4.32 mmol, 0.768 g) was then added drop-wise slowly over 10 min and the mixture was stirred at room temperature. After 4 h it was poured into a solution of water (100 mL) and dichloromethane (100 mL). The solution was neutralized with 5N sodium hydroxide aqueous solution, followed by extraction with dichloromethane. And the organic phase was dried over $MgSO_4$, filtered and evaporated under reduced pressure.

A mix of the crude product (3.414 mmol, 1.1 g), (4-(triphenylsilyl)phenyl)boronic acid (4.097 mmol, 1.558 g) and tetrakis(triphenylphosphine) palladium (0.171 mmol, 0.197 g) in 150 mL of THF and 75 mL 2N sodium carbonate aqueous solution was stirred at 75 ℃ for 18 h. After cooling to room temperature 100 mL water and 100 mL dichloromethane were added, followed by extraction with dichloromethane. And the organic phase was dried over $MgSO_4$, filtered and concentrated under reduced pressure to give a black solid, which was subjected to column chromatography on silica gel (ethyl acetate and *n*-hexane as eluent, 1:30, v/v, R_f = 0.3) to yield the target product of TPSPCz. The product was purified again by precipitation using dichloromethane and methanol to afford pure TPSPCz, white solid (0.530 g, 26.87 %). ^{1}H NMR(300MHz, $CDCl_3$, δ): 8.35–8.43 (s, 1H), 8.14–8.22 (d, 1H), 7.55–7.81 (m, 15H), 7.35–7.55 (m, 13H), 7.28–7.34 (m, 1H). ^{13}C NMR(300MHz, $CDCl_3$, δ): 142.79, 141.11, 140.28, 137.37, 136.68, 136.19, 134.11, 132.84, 131.68, 129.65,

129.34, 127.65, 127.28, 126.81, 126.48, 125.91, 125.20, 123.66, 123.21, 120.09, 119.86, 118.61, 109.82, 109.68. Elemental anal. calcd (%) for $C_{42}H_{31}NSi$: N, 2.42; C, 87.31; H, 5.41; Found: N, 2.39; C, 87.35; H, 5.43. GC-MS (EI): m/z(%) calcd. for $C_{42}H_{31}NSi$, 577.79; found, 577.9 (100).

3,6-dibromo-9-phenyl-carbazole (1) : A 9-phenyl-carbazole (6.165 mmol, 1.5 g) was dissolved in 100 mL of acetic acid and 120 mL of chloroform. *N*-bromosuccinimide (12.941 mmol, 2.304 g) was then added drop-wise slowly and the mixture was stirred at room temperature. After 4 h it was poured into a solution of water (100 mL) and dichloromethane (100 mL), followed by extraction with dichloromethane. And the organic phase was dried over $MgSO_4$, filtered and evaporated under reduced pressure. After removing the solvents the residue was purified by column chromatography on silica gel (ethyl acetate and *n*-hexane as eluent, 1:15, v/v, R_f = 0.3) to yield compound **1** (2.03 g, 82.10 %). ^1H NMR(300MHz, DMSO, δ): 8.55–8.65 (s, 2H), 7.52–7.75 (m, 7H), 7.28–7.38 (d, 2H).

9-phenyl-3,6-bis(4-(triphenylsilyl)phenyl)-carbazole (TPS_2PCz) : A mix of compound **1** (1.486 mmol, 0.596 g), (4-(triphenylsilyl)phenyl)boronic acid (3.27 mmol, 1.243 g) and tetrakis(triphenylphosphine) palladium (0.149 mmol, 0.172 g) in 50 mL of THF and 25 mL 2N sodium carbonate aqueous solution was stirred at 75 ℃ for 18 h. After cooling to room temperature 100 mL water and 100 mL dichloromethane were added, followed by extraction with dichloromethane. And the organic phase was dried over $MgSO_4$, filtered and concentrated under reduced

pressure to give a black solid, which was subjected to column chromatography on silica gel (ethyl acetate and *n*-hexane as eluent, 1:7, v/v, R_f = 0.3) to yield the target product of TPS_2PCz. The product was purified again by precipitation using dichloromethane and methanol to afford pure TPS_2PCz, white solid (0.550 g, 40.57 %). ^{1}H NMR(300MHz, $CDCl_3$, δ): 8.38–8.48 (s, 2H), 7.55–7.82 (m, 26H), 7.32–7.55 (m, 21H). ^{13}C NMR(500MHz, $CDCl_3$, δ): 143.15, 141.94, 137.18, 136.66, 134.56, 133.53, 132.23, 130.20, 129.82, 128.12, 127.86, 127.22, 126.94, 125.91, 124.26, 119.16, 110.48. Elemental anal. calcd (%) for $C_{66}H_{49}NSi_2$: N, 1.54; C, 86.89; H, 5.41; Found: N, 1.59; C, 86.94; H, 5.46. MS (MALDI-TOF): m/z(%) calcd. for $C_{66}H_{49}NSi_2$, 911.34 (100), 912.34 (81.9), 913.35 (25.6); found, 911.19 (100), 912.20 (90), 913.20 (55), 914.20 (25).

1,2-*trans*-di(carbazol-9-yl)cyclobutane (2) : A 9-vinylcarbazole (77.624 mmol, 15 g) was dissolved in 200 mL of acetone. And the solution was stirred at room temperature with Xe lamp and handled UV lamp. After 18 h it was evaporated under reduced pressure. After removing the solvents the residue was dissolved in dichlromethane, and then purified by precipitation using dichloromethane and methanol to afford pure compound **2** (7.7 g, 25.67 %). ^{1}H NMR(300MHz, $CDCl_3$, δ): 7.99–8.13 (d, 4H), 7.5–7.63 (d, 4H), 7.32–7.48 (t, 4H), 7.15–7.24 (t, 4H), 6.22–6.38 (m, 2H), 3.01–3.23 (m, 2H), 2.66–2.84 (m,2H).

1,2-*trans*-bis(3,6-dibromo-carbazol-9-yl)cyclobutane (3) : A compound **2** (5.175 mmol, 2 g) was dissolved in 300 mL of acetic acid and 500 mL of chloroform. *N*-bromosuccinimide (23.2865 mmol, 4.145 g) was then added drop-

wise slowly and the mixture was stirred at room temperature. After 4 h it was poured into a solution of water (150 mL) and dichloromethane (150 mL). The solution was neutralized with 5N sodium hydroxide aqueous solution, followed by extraction with dichloromethane. And the organic phase was dried over $MgSO_4$, filtered and evaporated under reduced pressure. The crude residue was purified by recrystallization from dichloromethane to afford pure compound **3**, white solid (2.74 g, 75.42 %). ^{1}H NMR(300MHz, $CDCl_3$, δ): 8.04–8.18 (s, 4H), 7.41–7.53 (d, 4H), 7.28–7.38 (d, 4H), 5.92–6.11 (m, 2H), 2.92–3.14 (m, 2H), 2.68–2.86 (m, 2H).

1,2-*trans*-bis(3,6-bis(4-(triphenylsilyl)phenyl)-carbazol-9-yl)cyclobutane (TPS$_4$DCz) : A mix of compound **3** (3.561 mmol, 2.11 g), (4-(triphenylsilyl)phenyl)boronic acid (17.092 mmol, 5.5 g) and tetrakis(triphenylphosphine) palladium (0.356 mmol, 0.348 g) in 200 mL of THF and 100 mL 2N sodium carbonate aqueous solution was stirred at 75 ℃ for 18 h. After cooling to room temperature 150 mL water and 150 mL dichloromethane were added, followed by extraction with dichloromethane. And the organic phase was dried over $MgSO_4$, filtered and concentrated under reduced pressure to give a black solid, which was subjected to column chromatography on silica gel (dichloromethane and *n*-hexane as eluent, 1:2, v/v, R_f = 0.3) to yield the target product of TPS$_4$DCz. The product was purified again by precipitation using dichloromethane and *n*-hexane to afford pure TPS$_4$DCz, white solid (1.740 g, 28.34 %). ^{1}H NMR(300MHz, $CDCl_3$, δ): 8.3–8.4 (s, 4H), 7.55–7.76 (m, 48H), 7.32–7.51 (m, 36H), 6.23–6.4 (m, 2H), 3.06–3.25 (m, 2H), 2.73–2.95 (m, 2H). ^{13}C NMR(500MHz, $CDCl_3$, δ): 142.88, 140.25, 137.17, 136.65, 134.56, 133.02, 132.29,

129.81, 128.11, 126.85, 125.77, 124.58, 119.36, 110.35, 55.11, 21.43. Elemental anal. calcd (%) for $C_{124}H_{94}N_2Si_4$: N, 1.62; C, 86.37; H, 5.49; Found: N, 1.61; C, 86.29; H, 5.49. MS (MALDI-TOF): m/z(%) calcd. for $C_{124}H_{94}N_2Si_4$, 1723.65 (100), 1722.65 (64.4), 1724.66 (58.6), 1725.66 (37.8); found, 1720.88 (100), 1722.88 (95), 1723.89 (83), 1719.88 (70).

II-4-3. Device Fabrication and Measurement

The device fabrication process firstly spin-coated aqueous solution of PEDOT:PSS at 1500 rpm for 40 s under nitrogen atmosphere to form the 40 nm hole-injection layer onto a pre-cleaned ITO (indium tin oxide) glass substrates and baked at 150 ℃ for 10 min. Next, an emitting layer was formed by using a solution-process. Various solutions that contained 8 wt% Ir(III) complexes (FIrpic, $Ir(PPy)_3$, $Ir(Piq)_2acac$) doped in TPS series and PVK, respectively, were prepared by dissolving the corresponding host and guest molecules in chlorobenzene. The solutions were spin-coated at 2000 rpm for 40s under nitrogen atmosphere to form 30 nm emitting layer. The resultant coated layers were subsequently heated at 100 ℃ for 30 min to remove residual solvent under nitrogen atmosphere. Finally, a BCP/Alq_3 as the electron-transporting layer (20 nm/30 nm), a cathode composed of LiF (1 nm) and Al (100 nm) was sequentially deposited onto the substrate at a base pressure < 5×10^{-7} Torr. Current density-voltage-luminance (*J-V-L*) characteristics, EL spectra, and CIE chromaticity coordinates of the PhOLEDs were measured simultaneously using a Keithley 237 programmable source meter and a SpectraScan PR650 (Photo Research). Assuming Lambertian emission, the external quantum efficiency (EQE) was calculated from the luminance, current density and electroluminescence spectrum.

II-5. References

1. C. W. Tang and S. A. VanSlyke, *Appl. Phys. Lett.*, 1987, **51**, 913.
2. B. W. D'Andrade and S. R. Forrest, *Adv. Mater.*, 2004, **16**, 1585.
3. (a) S. R. Forrest, *Nature*, 2004, **428**, 911; (b) A. R. Duggal, J. J. Shiang, M. H. Christian and F. F. Donald, *Appl. Phys. Lett.*, 2002, **80**, 3470; (c) B. C. Krummacher, V.-E. Choong, M. K. Mathai, S. A. Choulis, F. So, F. Jermann, T. Fiedler and M. Zachau, *Appl. Phys. Lett.*, 2006, **88**, 113506.
4. (a) M. A. Baldo, D. F. O'Brien, Y. You, A. Shoustikov, S. Sibley, M. E. Thompson and S. R. Forrest, *Nature*, 1998, **395**, 151; (b) Y. Kawamura, K. Goushi, J. Brooks, J. J. Brown, H. Sasabe and C. Adachi, *Appl. Phys. Lett.*, 2005, **86**, 71104; (c) C. Adachi, M. A. Baldo, M. E. Thompson and S. R. Forrest, *J. Appl. Phys.*, 2001, **90**, 5048; (d) Y. R. Sun, N. C. Giebink, H. Kanno, B. W. Ma, M. E. Thompson and S. R. Forrest, *Nature*, 2006, **440**, 908; (e) A. Köhler, J. Wilson and R. Friend, *Adv. Mater.*, 2002, **14**, 701; (f) T. Tsuzuki and S. Tokito, *Adv. Mater.*, 2007, **19**, 276; (g) S.-J. Su, E. Gonmori, H. Sasabe and J. Kido, *Adv. Mater.*, 2008, **20**, 4189; (h) L. Xiao, S. -J. Su, Y. Agata, H. Lan and J. Kido, *Adv. Mater.*, 2009, **21**, 1271.
5. (a) C. Adachi, M. A. Baldo, S. R. Forrest and M. E. Thompson, *Appl. Phys. Lett.*, 2000, **77**, 904; (b) J. S. Huang, M. Pfeiffer, A. Werner, J. Blochwitz, K. Leo and S. Y. Liu, *Appl. Phys. Lett.*, 2002, **80**, 39; (c) X. Yang, D. Müller, D. Neher and K. Meerholz, *Adv. Mater.*, 2006, **18**, 948; (d) X. Yang, D. Neher, D. Hertel and T. K. Däubler, *Adv. Mater.*, 2004, **16**, 161; (e) N. Rehmann, D. Hertel, K. Meerholz, H. Becker and S. Heun, *Appl. Phys. Lett.*, 2007, **91**,

103507.

6. (a) M. C. Gather, A. Köhnen, K. Meerholz, *Adv. Mater.*, 2011, **23**, 2; (b) J. Huang, G. Li, E. Wu, Q. Xu, Y. Yang, *Adv. Mater.*, 2006, **18**, 114; (c) X. Gong, H. Benmansour, G. C. Bazan and A. J. Heeger, *J. Phys. Chem. B*, 2006, **110**, 7344; (d) F. So, B. Krummacher, M. K. Mathai, D. Poplavskyy, S. A. Choulis and V.-E. Choong, *J. Appl. Phys.*, 2007, **102**, 091101; (e) X. Gong, W. Ma, J. C. Ostrowski, G. C. Bazan, D. Moses and A. J. Heeger, *Adv. Mater.*, 2004, **16**, 615; (f) H. Wu, L. Ying, W. Yang and Y. Cao, *Chem. Soc. Rev.*, 2009, **38**, 3391.
7. B. Park, Y. H. Huh, H. G. Jeon, C. H. Park, T. K. Kang, B. H. Kim and J. Park, *J. Appl. Phys.*, 2010, **108**, 094506.
8. (a) M. A. Baldo, C. Adachi and S. R. Forrest, *Phys. Rev. B: Condens. Matter Mater. Phys.*, 2000, **62**, 10967; (b) N. C. Giebink and S. R. Forrest, *Phys. Rev. B: Condens. Matter Mater. Phys.*, 2008, **77**, 235215; (c) Y. Kawamura, J. Brooks, J. J. Brown, H. Sasabe and C. Adachi, *Phys. Rev. Lett.*, 2006, **96**, 017404; (d) M. A. Baldo, S. Lamansky, P. E. Burrows, M. E. Thompson and S. R. Forrest, *Appl. Phys. Lett.*, 1999, **75**, 4; (e) D. F. O'Brien, M. A. Baldo, M. E. Thompson and S. R. Forrest, *Appl. Phys. Lett.*, 1999, **74**, 442.
9. Y. Tao, C. Yang and J. Qin, *Chem. Soc. Rev.*, 2011, **40**, 2943.
10. (a) M. F. Wu, S. J. Yeh, C. T. Chen, H. Murayama, T. Tsuboi, W. S. Li, I. Chao, S. W. Liu and J. K. Wang, *Adv. Funct. Mater.*, 2007, **17**, 1887; (b) Y. Shirota, *J. Mater. Chem.*, 2005, **15**, 75.
11. (a) R. J. Holmes, S. R. Forrest, Y.-J. Tung, R. C. Kwong, J. J. Brown, S. Garon, S. Garon and M. E. Thompson, *Appl. Phys. Lett.*, 2003, **82**, 2422; (b) S. Tokito, T. Iijima, Y. Suzuri, H. Kita, T. Tsuzuki and F. Sato, *Appl. Phys. Lett.*, 2003, **83**,

569; (c) S.-J. Yeh, M.-F. Wu, C.-T. Chen, Y.-H. Song, Y. Chi, M.-H. Ho, S.-F. Hsu and C. H. Chen, *Adv. Mater.*, 2005, **17**, 285; (d) M.-H. Tsai, H.-W. Lin, H.-C. Su, T.-H. Ke, C.-c. Wu, F.-C. Fang, Y.-L. Liao, K.-T. Wong and C.-I. Wu, *Adv. Mater.*, 2006, **18**, 1216; (e) M.-H. Tsai, Y.-H. Hong, C.-H. Chang, H.-C. Su, C. -c. Wu, A. Matoliukstyte, J. Simokaitiene, S. Grigalevicius, J. V. Grazulevicius and C.-P. Hsu, *Adv. Mater.*, 2007, **19**, 862; (f) P.-I. Shih, C.-L. Chiang, A. K. Dixit, C.-K. Chen, M.-C. Yuan, R.-Y. Lee, C.-T. Chen, E. W.-G. Diau and C.-F. Shu, *Org. Lett.*, 2006, **8**, 2799; (g) K.-T. Wong, Y.-M. Chen, Y.-T. Lin, H.-C. Su and C. -c. Wu, *Org. Lett.*, 2005, **7**, 5361; (h) D. R. Whang, Y. You, S. H. Kim, W.-l. Jeong, Y.-S. Park, J.-J. Kim and S. Y. Park, *Appl. Phys. Lett.*, 2007, **91**, 233501; (i) J. Ding, B. Zhang, J. Lü, Z. Xie, L. Wang, X. Jing and F. Wang, *Adv. Mater.*, 2009, **21**, 4983.

12. (a) R. J. Holmes, B. W. D'Andrade, S. R. Forrest, X. Ren, J. Li and M. E. Thompson, *Appl. Phys. Lett.*, 2003, **83**, 3818; (b) X. Ren, J. Li, R. J. Homes, P. I. Djurovich, S. R. Forrest and M. E. Thompson, *Chem. Mater.*, 2004, **16**, 4743; (c) P.-I. Shih, C.-H. Chien, C.-Y. Chuang, C.-F. Shu, C.-H. Yang, J.-H. Chen and Y. Chi, *J. Mater. Chem.*, 2007, **17**, 1692; (d) J.-J. Lin, W.-S. Liao, H.-J. Huang, F.-I. Wu and C.-H. Cheng, *Adv. Funct. Mater.*, 2008, **18**, 485; (e) S. H. Kim, J. Jang, S. J. Lee and J. Y. Lee, *Thin Solid Films*, 2008, **517**, 722.
13. (a) P.-I. Shih, C.-H. Chien, F.-I. Wu and C.-F. Shu, *Adv. Funct. Mater.*, 2007, **17**, 3514; (b) P. Marsal, I. Avilov, D. A. S. Filho, J. L. Bredas and D. Beljonne, *Chem. Phys. Letter.*, 2004, **392**, 521.
14. (a) P. A. Vecchi, A. B. Padmaperuma, H. Qiao, L. S. Sapochak and P. E. Burrows, *Org. Lett.*, 2006, **8**, 4211; (b) A. B. Padmaperuma, L. S. Sapochak

and P. E. Burrows, *Chem. Mater.*, 2006, **18**, 2389; (c) L. S. Sapochak, A. B. Padmaperuma, X. Cai, J. L. Male and P. E. Burrows, *J. Phys. Chem. C*, 2008, **112**, 7989; (d) S. O. Jeon, K. S. Yook, C. W. Joo and J. Y. Lee, *Appl. Phys. Lett.*, 2009, **94**, 013301.

15. (a) G. E. Johnson, *J. Chem. Phys.*, 1975, **62**, 4697; (b) M. Pope and C. E. Swenberg, *Electronic Processes in Organic Crystal*, Oxford University Press, New York (1982).
16. M. J. Frisch, G. W. Trucks, H. B. Schlegel, G. E. Scuseria, M. A. Robb, J. R. Cheeseman, G. Scalmani, V. Barone, B. Mennucci, G. A. Petersson, H. Nakatsuji, M. Caricato, X. Li, H. P. Hratchian, A. F. Izmaylov, J. Bloino, G. Zheng, J. L. Sonnenberg, M. Hada, M. Ehara, K. Toyota, R. Fukuda, J. Hasegawa, M. Ishida, T. Nakajima, Y. Honda, O. Kitao, H. Nakai, T. Vreven, J. A. Montgomery, Jr., J. E. Peralta, F. Ogliaro, M. Bearpark, J. J. Heyd, E. Brothers, K. N. Kudin, V. N. Staroverov, R. Kobayashi, J. Normand, K. Raghavachari, A. Rendell, J. C. Burant, S. S. Iyengar, J. Tomasi, M. Cossi, N. Rega, J. M. Millam, M. Klene, J. E. Knox, J. B. Cross, V. Bakken, C. Adamo, J. Jaramillo, R. Gomperts, R. E. Stratmann, O. Yazyev, A. J. Austin, R. Cammi, C. Pomelli, J. W. Ochterski, R. L. Martin, K. Morokuma, V. G. Zakrzewski, G. A. Voth, P. Salvador, J. J. Dannenberg, S. Dapprich, A. D. Daniels, O. Farkas, J. B. Foresman, J. V. Ortiz, J. Cioslowski and D. J. Fox, *Gaussian 09*, Revision A.01, Gaussian Inc., Wallingford CT, 2009.
17. (a) F. Santerre, I. Bedjia and J. P. Dodelet, *Chem. Mater.*, 2001, **13**, 1739; (b) G. S. Liou, S. H. Hsiao, W. C. Chen and H. J. Yen, *Macromolecules*, 2006, **39**, 6036.

18. S.-P. Huang, T.-H. Jen, Y.-C. Chen, A.-E. Hsiao, S.-H. Yin, H.-Y. Chen and S.-A. Chen, *J. Am. Chem. Soc.*, 2008, **130**, 4699.
19. M. H. Tsai, T. H. Ke, H. W. Lin, C. C. Wu, S. F. Chiu, F. C. Fang, Y. L. Liao, K. T. Wong, Y. H. Chen and C. I. Wu, *ACS Appl. Mater. Interfaces*, 2009, **1**, 567.
20. K. Brunner, A. van Dijken, H. Börner, J. J. A. M. Bastiaansen, N. M. M. Kiggen and B. M. W. Langeveld, *J. Am. Chem. Soc.*, 2004, **126**, 6035.
21. (a) C. Du, S. Ye, J. Chen, Y. Guo, Y. Liu, K. Lu, Y. Liu, T. Qi, X. Gao, Z. Shuai and G. Yu, *Chem. Eur. J.*, 2009, **15**, 8275; (b) Z. Ge, T. Hayakawa, S. Ando, M. Ueda, T. Akiike, H. Miyamoto, T. Kajita and M.-a. Kakimoto, *Adv. Funct. Mater.*, 2008, **18**, 584.

초록

Tetraphenylsilane 기를 포함하여 용액 공정이 가능한 고효율 인광 유기전계발광소자 단분자 호스트 물질에 관한 연구

조 명 현

공과대학 재료공학부

서울대학교 대학원

본 논문에서는 고효율의 인광 유기전계발광소자를 목표로 하여, 테트라페닐실란 (Tetraphenylsilane) 기를 포함함으로써 용액 공정이 가능해지는 새로운 단분자 호스트 물질군을 보고하였다. 새로이 개발된 이 물질군은 TPS series 라 명명되었으며, 9-phenyl-3-(4-(triphenylsilyl)phenyl)-carbazole (TPSPCz), 9-phenyl-3,6-bis(4-

(triphenylsilyl)phenyl)-carbazole (TPS_2PCz), 1,2-*trans*-bis(3,6-bis(4-(triphenylsilyl)phenyl)-carbazol-9-yl)cyclobutane (TPS_4DCz) 등 세 물질로 구성되어 있다. 카바졸의 C3, C6 위치에 수소 대신 테트라페닐실란기가 치환됨으로써 용액 공정을 통해 균일한 필름을 얻는 것이 가능해졌다. 또한 광물리적, 필름의 형태학적 특성 연구에 기초하여, 부피가 크고 상당히 뒤틀려 있는 형태의 테트라페닐실란기가 가지는 공간상 분리 효과에 의하여 동일 평면상에 위치하는 카바졸의 엑시머 형성이 효과적으로 억제된다는 것을 증명하였다. 위 호스트 물질들은 테트라페닐실란기의 수가 증가할수록 더욱 높은 열분해 온도(전체 무게 중 약 5%의 무게가 줄어드는 온도)를 갖는 현상을 보였다 (TPSPCz : 363 ℃, TPS_2PCz : 424 ℃, TPS_4DCz : 472 ℃). 특히 *fac*-tris(2-phenylpyridine) iridium (III) ($Ir(PPy)_3$) 가 게스트, TPS_4DCz 가 호스트로 쓰인 인광 유기전계발광소자의 경우, $Ir(PPy)_3$ 가 게스트, PVK 가 호스트로 쓰인 인광 유기전계발광소자와 비교하였을 때 최대 154 % 까지 향상된 소자 성능을 보여주었다.

주요어 : 테트라페닐실란, 용액 공정, 단분자, 호스트, 인광, 전기인광, 유기전계발광소자

학번 : 2010-20632

LIST OF PRESENTATIONS

1. Myung-Hyun Jo[1], Dong Ryeol Whang[1], Se Hun Kim[1], Jungjin Yang[2], Changhee Lee[2], and Soo Young Park[1]*, “Triphenylsilane containing solution-processable small-molecular host for highly efficient phosphorescent organic light-emitting diodes”, KJF-ICOMEP 2011, Sep 15-19, 2011, Gyeongju, Korea.